SiliconPV 2025, 15th International Conference on Crystalline Silicon Photovoltaics
Advances in Industrial Silicon Solar Cells
https://doi.org/10.52825/siliconpv.v3i.2690

Published: 20 Jan. 2026

Thermally Stable Epiwafers for PV Applications

Rabin Basnet[1,*], Clemens Winter[2], Nicole Bein[2], Matthias Heilig[2], Frank Siebke[2], Giuliano Vescovi[2], and Daniel Macdonald[1]

[1]School of Engineering, The Australian National University, Australia

[2]NexWafe GmbH, Germany

*Correspondence: Rabin Basnet, rabin.basnet@anu.edu.au

Abstract. This work assesses the thermal stability of *n*-type Epiwafers after a boron diffusion based on the carrier lifetime measurements and photoluminescence images. The Epiwafers show a high bulk quality (iV_{oc} > 735-745 mV) in their initial state after passivation with PECVD SiN_x:H films. After a customized thermal budget for boron diffusion, the Epiwafers did not show any significant degradation, suggesting their high thermal stability. In contrast, some n-type Czochralski (nCz) silicon control samples degraded significantly (ΔiV_{oc} = -30 mV) due to the formation of ring defects during boron diffusion.

Keywords: Epiwafers, Boron-Diffusion, Thermal-Stability

1. Introduction

Epitaxially grown wafer (Epiwafers) are considered a promising alternative to conventional silicon wafers for photovoltaic (PV) applications, primarily due to their low carbon footprint in the current electricity mix and kerfless manufacturing process [1], [2]. In addition to environmental benefits, Epiwafers offer cost-reduction potential, however, their production throughput must be improved to match that of a Czochralski (Cz) ingot process. Epiwafers typically exhibit lower oxygen than conventional Cz wafers [1], reducing the formation of oxygen-related bulk defects during high-temperature processes.

New Recently, NexWafe's EpiNex™ solar wafers achieved 24.4% efficiency with a commercial M6 silicon heterojunction (SHJ) cell [3]. However, for high-temperature solar cell fabrication, such as tunnel oxide passivated contact (TOPCon), the thermal stability of Epiwafers remains an important question. Previously, Rittmann *et al.* [2] reported an efficiency potential > 25% for *p*-type Epiwafers using a doped poly-Si passivating contact structure. Their study examined the impact of 1050°C oxidation for 1 hour on Epiwafers and observed partial degradation in 4-inch wafers. While large areas retained excellent carrier lifetimes, reduced lifetimes were detected around slip lines. The degradation was attributed to either the dissociation of impurities clustered at slip lines during oxidation or the multiplication and propagation of dislocations within these regions [4].

This work investigates the thermal stability of *n*-type EpiNex™ from NexWafe, particularly under a high-temperature boron diffusion, and compares their performance with conventional *n*-type industrial Cz wafers.

2. Experimental details

Three groups of *n*-type silicon wafers were used in this work. The first group of samples were *n*-type Epiwafers subjected to a phosphorus-diffusion gettering step, with the diffused regions etched off. The remaining two groups were also *n*-type wafers but conventional Czochralski-grown silicon (Cz-Si) wafers (referred as nCz1 and nCz2) from two different ingot growers. The wafer properties of these samples are presented in Table 1. The interstitial oxygen concentrations ($[O_i]$) of the Cz wafers were measured at room temperature using Fourier-transform infrared (FTIR) spectroscopy. However, the $[O_i]$ in the Epiwafers could not be accurately determined due to their low thickness and inherently low oxygen content. Therefore, reference $[O_i]$ values for comparison with Cz wafers are used from Rittmann et al.[2] on p-type Epiwafers, which is lower than in the conventional Cz wafers. Note the nCz1 wafers were from commercially available wafer stock (ingot position was not available), while the nCz2 wafers were from a seed-end of a standard silicon ingot.

***Table 1**. Wafer properties of the samples used in this work.*

Samples	Thickness (µm)	Resistivity (Ω·cm)	$[O_i]$ (cm^{-3})
Epiwafers	110 ± 10	1-1.2	$(0.1\text{-}4) \times 10^{17}$ [2]
nCz1	240 ± 10	1.5	4×10^{17}
nCz2	135 ± 5	5-6	7×10^{17}

Figure 1 shows the detailed experimental outline used in this work. Both types of *n*-type Cz-Si wafers underwent a phosphorus diffusion gettering (PDG) step to be comparable with the initial state of the Epiwafers with the diffused surfaces etched off prior to further processing. Then, all the samples were passivated by depositing $70\ nm$ thick SiN_x:H layers on both sides using Plasma Enhanced Chemical Vapor Deposition (PECVD) (Roth and Rau AK400) with a substrate temperature ranging from $250 - 300\ ℃$ to assess their initial material quality and are referred as “initial (post-gettering)”. Following this, the SiN_x:H layers on all samples were etched away using an HF dip, and a short TMAH etch was performed to refresh the surface.

Next, all the samples were annealed at 650°C for 2.5 hours in nitrogen to accelerate oxygen precipitation. This annealing was utilized to accelerate the formation of oxygen precipitation nuclei [5], [6] and induce ring defects in the subsequent boron diffusion process. Boron diffusion was performed at 900°C for 30 minutes with BBr_3 as the dopant source, followed by a 40-minute drive-in in nitrogen and a 20-min oxidation at 950°C, resulting in a sheet resistance of 150-160 Ω/□. Then, all the diffused layers were etched off using TMAH etching and all the samples were passivated by the same PECVD-deposited SiN_x:H as for the initial state. Note that standard RCA cleaning was performed on the samples before any high-temperature processing.

Effective carrier lifetimes were measured using the quasi-steady state photoconductance and transient photoconductance decay techniques with a WCT-120 tool from Sinton Instruments [7]. PL images were captured using an LIS-R1 PL imaging tool from BT imaging [8].

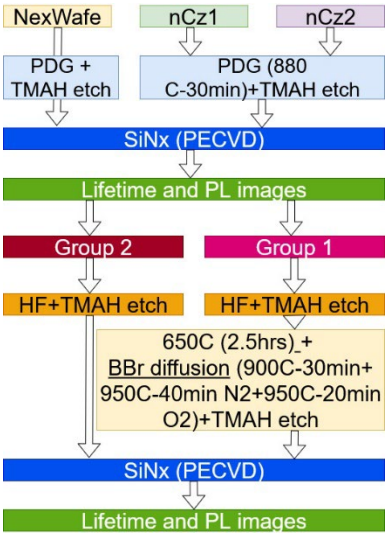

Figure 1. *Experimental outline used in this work.*

3. Results and discussion

3.1 Initial (post-gettering)

Figure 2 shows the effective lifetimes (at $\Delta n = 1 \times 10^{15}$ cm^{-3}) and the implied open circuit voltages (iV_{oc}) at 1-sun condition for the three types of samples after gettering, which represents the "initial state" in this work. The initial effective lifetimes of the samples range from $2.2 - 4.5$ ms ($740 - 745$ mV), $9 - 12.5$ ms ($730 - 735$ mV) and $9 - 12$ ms ($735 - 740$ mV) for the Epiwafer, nCz1 and nCz2, samples respectively. The lower effective lifetimes of Epiwafers compared to nCz wafers is related to their low thickness and resistivities, as shown in Table 1, which makes iV_{oc} values comparable to the nCz2 samples.

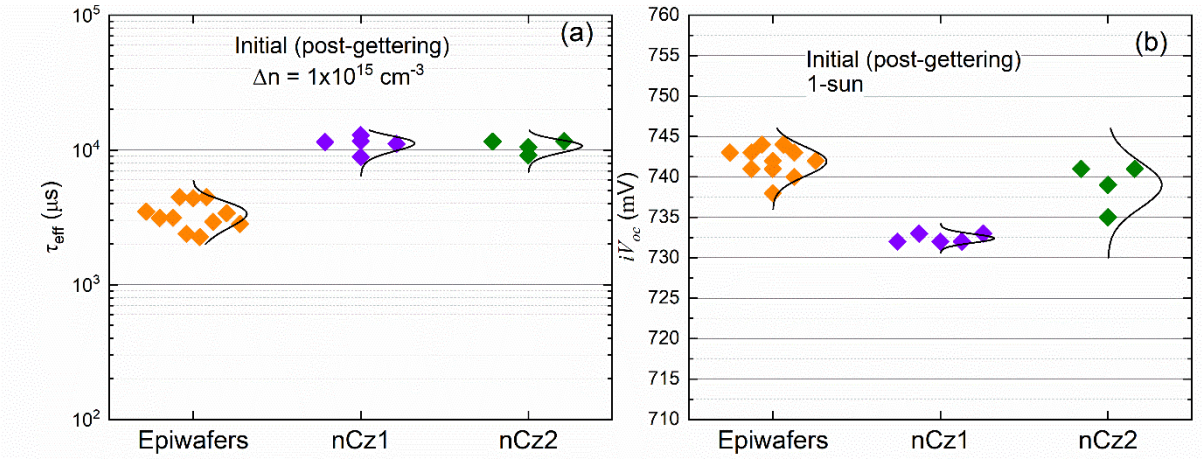

Figure 1. *(a) Effective lifetimes (at Δn=1×10^15 cm-3) and (b) iVoc (at 1-sun) of the three types of samples used in this work in their initial state (post gettering).*

3.2 After boron diffusion

Figure 3 shows the injection-dependent carrier lifetimes of representative samples from the three types of samples, both before and after boron diffusion step. The variations in effective lifetimes at the initial state (post-gettering) can be partly attributed to differences in the resistivity and thickness of the wafers (Table 1), as also reflected in the intrinsic carrier lifetimes derived from the Niewelt model [9]. After boron diffusion, the effective lifetimes of the Epiwafers

did not show any significant degradation (Figure 3 (a)). In contrast, the nCz samples exhibited some degradation, with the nCz2 samples showing a significant reduction in carrier lifetimes (Figure 3 (b) and (c)). Furthermore, the nCz samples experienced a reduction in both iV_{oc} and the implied voltage at the maximum power point (iV_{mpp}), as shown in Figure 3 (d). These results suggest that Epiwafers exhibit high stability against thermal degradation, primarily due to the absence of defects related to oxygen precipitation.

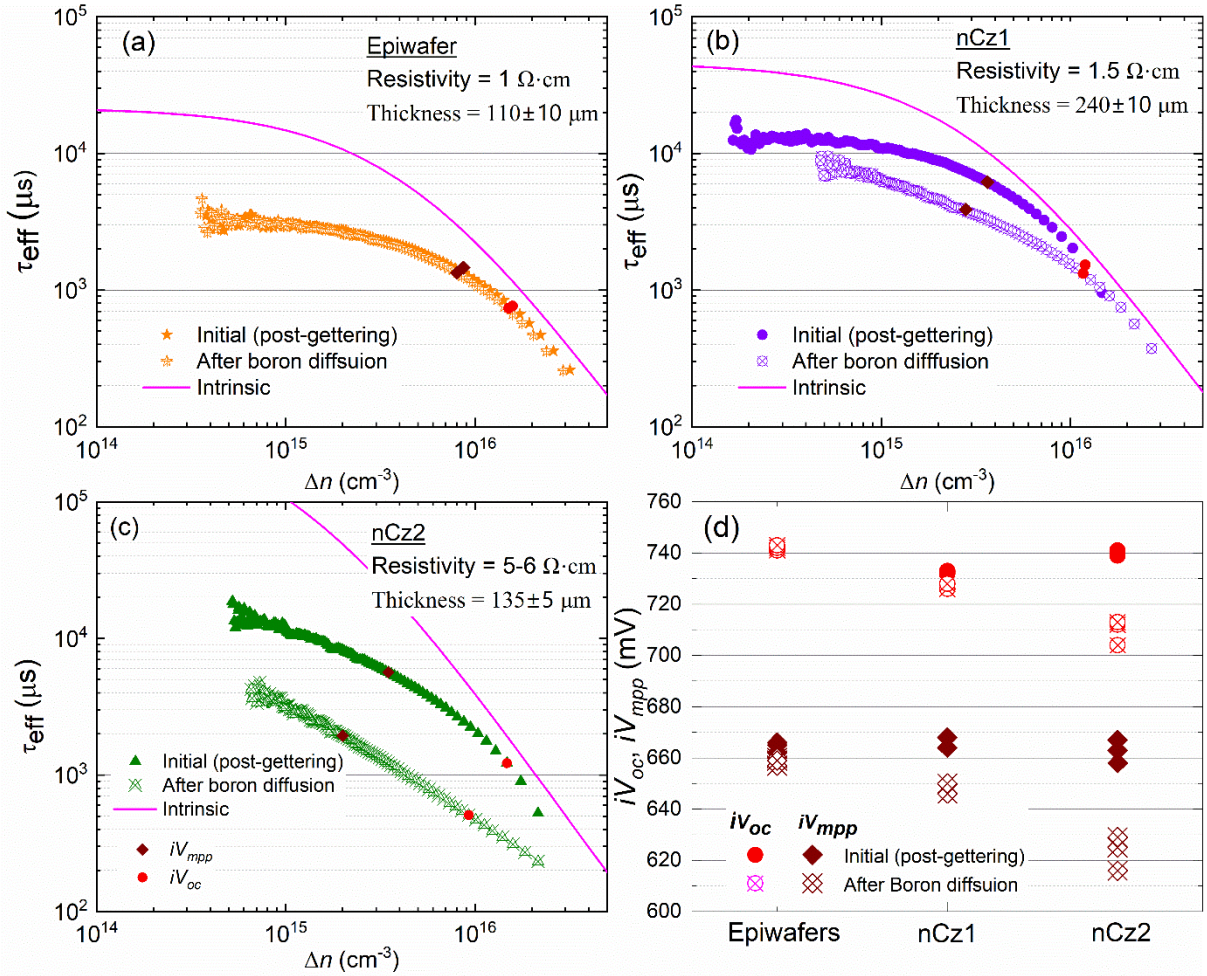

Figure 2. *Injection dependent carrier lifetimes of the representative (a) Epiwafers, (b) nCz1 and (c) nCz2 samples in the initial (post-gettering) state and after boron diffusion. (d) Comparison of iVoc (1-sun) and the iVmpp of the samples before and after boron.*

PL images also confirmed that no significant thermal degradation was observed in the Epiwafers, as shown in Figure 4. Note that some local non-uniformities due to processing-induced damage were observed in the samples. Both types of nCz-Si samples show some degradation, with nCz2 exhibiting clear ring defect formation. These wafers are from the seed-end of an ingot with relatively high [O_i], leading to the formation of ring defects by enhanced oxygen precipitation [10]. It is worth noting that the degree of degradation depends on the thermal budget, so these wafers may degrade further when used in industrial TOPCon fabrication, which includes front boron diffusion and rear n^+ poly-Si formation. It is worth noting that recent industrial *n*-type Cz wafers have achieved a high bulk lifetimes approaching their Auger limit, and contains low [O_i] < 4×10^{17} cm^{-3}, ensuring excellent thermal stability [11].

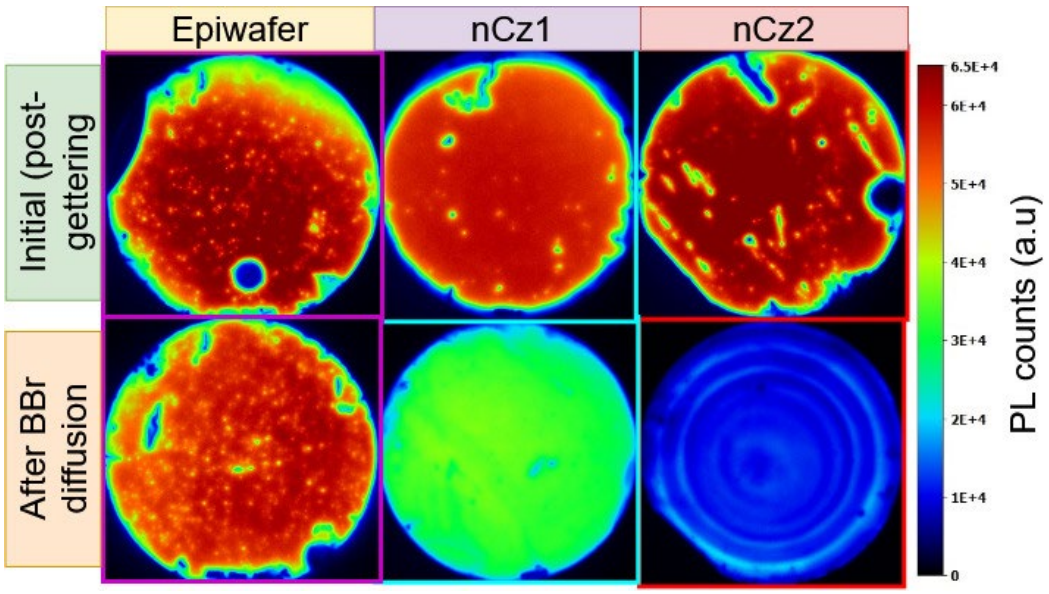

Figure 3. *Uncalibrated PL images of the n-type samples before and after boron diffusion and passivated by SiNx layers. All PL images were captured at 0.5suns illumination intensity for 0.5s.*

4. Conclusion

This work demonstrates that *n*-type Epiwafers exhibit excellent thermal stability during a customized high-temperature boron diffusion process. No significant degradation in carrier lifetimes or iV_{oc} was observed, as confirmed by PL imaging and lifetime measurements. In contrast, conventional *n*-type Cz wafers, especially those with higher interstitial oxygen concentrations, exhibit degradation due to oxygen precipitation-induced ring defects. These results highlight the suitability of Epiwafers for advanced high-temperature cell architectures like TOPCon, offering a promising pathway toward low-carbon, high-efficiency solar cells.

Data Availability

Data will be available upon a reasonable request

Author contributions

Rabin Basnet: Writing – review & editing, Writing – original draft, Validation, Methodology, Investigation, Formal analysis, Data curation, **Clemens Winter**: Resources, **Nicole Bein**: Resources, Writing – review & editing, **Matthias Heilig**: Resources, Frank Siebke: Resources, **Giuliano Vescovi**: Conceptualization, Resources, Writing – review & editing, Formal analysis and **Daniel Macdonald:** Writing – review & editing, Supervision, Project administration, Funding acquisition, Formal analysis.

Competing interests

RB and DM declare that they have no competing interests. CW, NB, MH, FS, and GV works with NexWafe which aim to commercialize Epwafers.

Funding

This work has been funded by NexWafe.

Acknowledgement

RB would like to acknowledge Christian Samundsett for help in sample processing. This work is supported by the Australian Renewable Energy Agency (ARENA) through the Australian Center for Advanced Photovoltaics (ACAP).

References

[1] C. Rittmann et al., “Toward Highly Efficient Low-Carbon Footprint Solar Cells: Impact of High-Temperature Processing on Epitaxially Grown p-Type Silicon Wafers,” Sol. RRL, vol. 8, no. 4, Feb. 2024, doi: 10.1002/solr.202300882.

[2] C. Rittmann et al., “Epitaxially Grown p-type Silicon Wafers Ready for Cell Efficiencies Exceeding 25%,” Sol. RRL, vol. 7, no. 8, Apr. 2023, doi: 10.1002/solr.202200698.

[3] NexWafe, “NexWafe Hits Key Milestones in Solar Efficiency and Scalability,” 2024.

[4] G. Coletti et al., “Impact of Metal Contamination in Silicon Solar Cells,” Adv. Funct. Mater., vol. 21, no. 5, pp. 879–890, Mar. 2011, doi: 10.1002/adfm.201000849.

[5] R. Basnet, M. Siriwardhana, H. T. Nguyen, and D. Macdonald, “Impact of Gettering and Hydrogenation on Sub-Band-Gap Luminescence from Ring Defects in Czochralski-Grown Silicon,” ACS Appl. Energy Mater., vol. 4, no. 10, pp. 11258–11267, Oct. 2021, doi: 10.1021/acsaem.1c02100.

[6] K. F. Kelton, R. Falster, D. Gambaro, M. Olmo, M. Cornara, and P. F. Wei, “Oxygen precipitation in silicon: Experimental studies and theoretical investigations within the classical theory of nucleation,” J. Appl. Phys., vol. 85, no. 12, pp. 8097–8111, Jun. 1999, doi: 10.1063/1.370648.

[7] R. A. Sinton and A. Cuevas, “Contactless determination of current-voltage characteristics and minority-carrier lifetimes in semiconductors from quasi-steady-state photoconductance data,” Appl. Phys. Lett., vol. 69, no. 17, pp. 2510–2512, 1996, doi: 10.1063/1.117723.

[8] T. Trupke, R. Bardos, M. Schubert, and W. Warta, “Photoluminescence imaging of silicon wafers,” Appl. Phys. Lett., vol. 89, no. 4, pp. 44107–44107, 2006, doi: 10.1063/1.2234747.

[9] T. Niewelt et al., “Reassessment of the intrinsic bulk recombination in crystalline silicon,” Sol. Energy Mater. Sol. Cells, vol. 235, p. 111467, Jan. 2022, doi: 10.1016/j.solmat.2021.111467.

[10] R. Basnet, C. Sun, H. Wu, H. T. Nguyen, F. E. Rougieux, and D. Macdonald, “Ring defects in n-type Czochralski-grown silicon: A high spatial resolution study using Fourier-transform infrared spectroscopy, micro-photoluminescence, and micro-Raman,” J. Appl. Phys., vol. 124, no. 24, Dec. 2018, doi: 10.1063/1.5057724.

[11] A. Kashizadeh et al., “Auger-limited bulk lifetimes in industrial Czochralski-grown n-type silicon ingots with melt recharging,” Sol. Energy Mater. Sol. Cells, vol. 277, p. 113143, Oct. 2024, doi: 10.1016/j.solmat.2024.113143.